

Information-Theoretic Detection of Bimanual Interactions for Dual-Arm Robot Plan Generation

Elena Merlo, Marta Lagomarsino, and Arash Ajoudani

Abstract—Programming by demonstration is a strategy to simplify the robot programming process for non-experts via human demonstrations. However, its adoption for bimanual tasks is an underexplored problem due to the complexity of hand coordination, which also hinders data recording. This paper presents a novel one-shot method for processing a single RGB video of a bimanual task demonstration to generate an execution plan for a dual-arm robotic system. To detect hand coordination policies, we apply Shannon’s information theory to analyze the information flow between scene elements and leverage scene graph properties. The generated plan is a modular behavior tree that assumes different structures based on the desired arms coordination. We validated the effectiveness of this framework through multiple subject video demonstrations, which we collected and made open-source, and exploiting data from an external, publicly available dataset. Comparisons with existing methods revealed significant improvements in generating a centralized execution plan for coordinating two-arm systems.

Index Terms—Semantic Scene Understanding, Bimanual Manipulation, Learning from Demonstration

I. INTRODUCTION

DESPITE the growing evidence of the benefits robots bring to industrial, healthcare, and domestic settings, such as increased productivity and enhanced well-being [1], robot programming remains the domain of expert programmers, hindering a wider adoption and use of such platforms.

Programming by Demonstration (PbD) has shown to be effective in making robot programming more accessible and intuitive [2]. Through hands-on demonstrations, PbD leverages the natural social learning process of mimicking others [3]. Typically, when a person performs a manual task, both hands are engaged, either actively, such as when carrying a bulky object, or with one hand assisting the other in performing the primary work [4]. For example, when writing, one hand holds the paper steady while the other moves the pen. Similarly, when stirring a cup, one hand supports the cup while the other stirs. In the literature, the problem of dual-arm manipulation programming is extensively treated [5], however, the adoption of PbD methods for bimanual tasks remains underexplored. That is partly due to the complexity of capturing and analyzing coordination features between the hands and the challenges associated with recording data from demonstrations.

A widely used PbD strategy is Kinesthetic Teaching (KT), which allows a demonstrator to physically guide the manipulator within its workspace through haptic interaction

Manuscript received: November 4, 2024; Revised: January 2, 2025; Accepted: March 5, 2025. This paper was recommended for publication by Editor Júlia Borràs Sol upon evaluation of the Associate Editor and Reviewers’ comments.

This work was supported by the European Union Horizon Project TORNADO (GA 101189557). The authors are with Human-Robot Interfaces and Interaction (HRII) Laboratory, Istituto Italiano di Tecnologia, Genoa, Italy. Elena Merlo is also with the Dept. of Informatics, Bioengineering, Robotics, and Systems Engineering, University of Genoa, Genoa, Italy. Corresponding author’s email: elena.merlo@iit.it.

Digital Object Identifier (DOI): see top of this page.

[3]. During this process, the robot’s onboard sensors record its states, generating data that enables the replication of the demonstrated trajectories [6]. While KT simplifies the correspondence problem [7], the quality of the demonstration heavily depends on the smoothness and dexterity of the human user, which is particularly difficult to maintain during bimanual activities that require moving two arms simultaneously. In [8], [9], the authors managed to transfer bimanual skills, such as handling objects like tubes or large dice, by applying KT on both arms of small-sized humanoid robots, leveraging their compact form.

To streamline the demonstration phase, robots can be instructed to replicate actions performed by an external person through a technique known as Observational Learning (OL) [10]. This method utilizes systems to capture human movements accurately. In [11], human arms’ movements and object displacements were recorded using Optitrack and analyzed offline to generate corresponding robot motions. Sensor-equipped gloves have been additionally used in [12] to monitor even individual finger movements. Although practical markerless and RGB-camera-based motion capture systems have been explored [13], the data they provide and process still lack the precision required for low-level PbD.

Recently, there has been growing interest in enabling robots to move beyond replicating demonstrated trajectories and gain *higher-level* semantic understanding of human behavior [14]. This includes recognizing (i) the task goal, (ii) the sequence of required skills, and (iii) the environmental conditions necessary for successful execution [15]. Such abstraction facilitates the generation of informed execution plans, improving robot decision-making [16]. However, these advancements predominantly focus on unimanual actions. For instance, in [17], a graph-based structure models the hands-objects relations and trains a network to classify actions for each hand independently. While effective for unimanual tasks, this approach oversimplifies bimanual activities, as hand actions are often interconnected. Although many studies have explored hand coordination [18]–[20], less attention is paid toward methods for automatically identifying bimanual activities from human motion data to enhance dual-arm robotic manipulation.

This work presents a novel method to identify bimanual interactions and coordination from a single RGB video demonstration of a manipulation task and automatically generate a robot plan to map human actions into robot commands. Compared to the state-of-the-art, our primary contribution lies in the application of Shannon’s Information Theory (IT) [21] to characterize bimanual activities. Our analysis of information flows enables us to recognize hand coordination policies, inspired by the taxonomy established in [20], and define the collaboration modalities for robotic arms. Our second contribution consists of providing a direct mapping to a modular

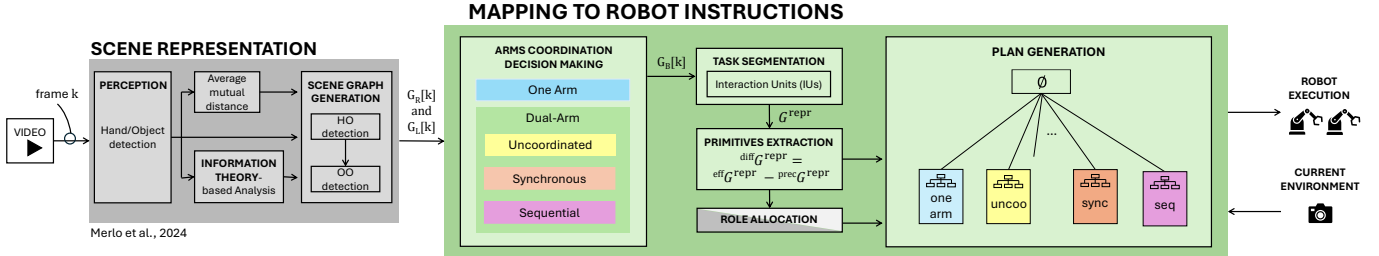


Fig. 1. Framework overview. The first block maps each video frame k into graphs $G_R[k], G_L[k]$ capturing task-relevant interactions for each hand, while the second block translates these into robot instructions, identifying arm coordination mode, extracting action sequences, and generating a dual-arm execution plan.

execution plan for a dual-arm system to enable it to replicate the demonstrated activity. The proposed framework builds on our previous work [22] to convert unimanual video demonstrations into time series of graphs that encode hand-object relations, including poses, distances, and shared information (see gray block in Fig. 1). The novelty compared to [22] lies in extending this framework to accommodate bimanual activities, through the design of the green block in Fig. 1. Specifically, the first contribution involves analyzing the topology of the graphs encoding bimanual interactions and the informational content of their elements to determine the coordination mode of the two hands. Without this capability, the system would generate separate, uncoordinated plans for each arm, which are inadequate for tasks requiring close coordination and precise sequencing of the hands' action. The second contribution involves the automatic generation of a Behavior Tree (BT) [23] that guides the dual-arm system replica. Depending on arms' coordination, the BT adopts a diverse structure to manage the execution of coordinated movements and provide a solution for the role allocation problem, avoiding conflicting actions and ensuring logical execution. The framework was tested on video demonstrations from two datasets and the retrieved task structure was compared with the one in [17].

II. METHODS

Our algorithm consists of two main blocks: Scene Representation and Mapping to Robot Instructions, as illustrated in Fig. 1. The first block transforms each video frame into graphs capturing interactions between scene elements. We used IT-based measures to effectively extract the active part of the scene, i.e., the task-relevant elements, and create a compact and reliable scene representation. The second block translates these representations into an execution plan for the dual-arm system, identifying the arms' coordination mode and extracting the actions required. This pipeline enables intuitive robot programming by automatically generating structured instructions to replicate the observed demonstration.

A. Scene Graph Generation

This section summarizes how hand activity in each frame k is mapped into a scene graph $G[k]$ [24]. In bimanual tasks, two independent graphs are generated per frame: $G_R[k]$ for the right hand and $G_L[k]$ for the left hand. A perception module captures the 6D pose of each object $o \in O$ and of the hands $\{R, L\}$ in the scene, which constitute the nodes of the scene graphs. The positional data are then processed to evaluate the informational content of each signal and the amount of information shared between elements. Positional signals are also analyzed to obtain

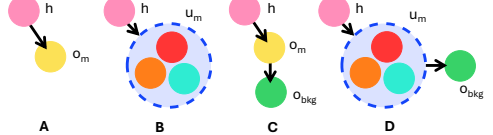


Fig. 2. Possible topologies for G_R and G_L encoding single-hand interactions: (A) hand h interacting with the manipulated object o_m ; (B) hand manipulating a unity of three objects u_m ; (C) interaction between o_m and a static background object o_{bkg} ; (D) u_m interacting with o_{bkg} .

elements' relative distances. These outputs are used to connect nodes in $G_R[k]$ and $G_L[k]$. For more details on this process, refer to [22].

1) *Scene Graph Topology*: Since graphs encode only the active part of the scene, $G_R[k]$ and $G_L[k]$ can assume one topology among those shown in Fig. 2. In the graph, there is always a hand node (h), representing the right hand in G_R and the left hand in G_L . The hand node can be connected to an object node o_m (as seen in topologies A and C). This signifies a hand-object interaction (HO), indicating they share information during manipulation. Alternatively, the hand might interact with a unity of objects u_m (as shown in topologies B and D). In these cases, the hand shares information with multiple objects simultaneously, such as when manipulating assembled objects or a box containing several items. The object or unity being manipulated can also interact with another stationary object in the background o_{bkg} , as shown in topologies C and D. This static object-object interaction (OO) occurs when the information flow between the two elements reaches a state of equilibrium. An example is placing a pen inside a case, leading to the OO between the pen and the case. The oriented edges show that the graph generation process starts from the hand, which is the active element causing changes in the environment, and each edge contains the relative position between the element at the tail w.r.t. the element at the tip.

2) *Information Theory Metrics in Manipulation Task*: To determine if two elements in the scene captured by frame k are sharing information (e.g., a hand and an object to establish a HO), we use *Mutual Information* (MI). This measure, derived from Shannon's IT, is applied to positional signals X and Y of a pair of scene elements, considering a time interval w centered in t^* , instant when frame k was taken. $MI(X(t^*) : Y(t^*))$ is defined as:

$$MI(X(t^*) : Y(t^*)) = \sum_{x \in \Omega_x} \sum_{y \in \Omega_y} p_{xy}(x,y) \cdot \log_2 \frac{p_{xy}(x,y)}{p_x(x)p_y(y)}, \quad (1)$$

where x and y are discrete measurements of X and Y from Ω_x and Ω_y , respectively, occurred within w ; $p_x(x)$ represents the probability of X taking value x , $p_y(y)$ of Y taking value

y , and $p_{xy}(x,y)$ is the joint probability of X and Y taking values x and y simultaneously. If $MI(X(t^*):Y(t^*)) = 0$, it indicates that in k the two elements are moving independently; otherwise, they are jointly moving. To recognize a manipulated unity u_m , we measure the shared information among the objects involved using *Co-Information*, which extends MI to multiple variables [25]. This approach provides a more reliable alternative to contact estimation or distance measurements, preventing interaction misidentification based only on proximity. Moreover, it captures motion dependencies more effectively than velocity analysis due to a quantitative assessment of information flow, even with less accurate or noisy perception data [22]. Note that the value of MI between a hand and the manipulated object during a *HO* is stored in the graph as an attribute of the corresponding edge. Finally, to identify a static *OO*, we monitor the informational content of the distance between o_m and o_{bkg} by computing its entropy over time $H(\bar{d}_{o_m, o_{bkg}}(t))$. A drop suggests the objects' relative position is stabilizing, thus their interaction is relevant.

B. Arms Coordination Decision Making

The first step towards generating the execution plan is recognizing the roles the two hands played in the human demonstration by analyzing the relations between the information flows originating from the two hands during bimanual tasks. This allows us to design the plan to reproduce the same coordination modality between the two robotic arms. The defined coordination modalities cover the majority of bimanual tasks, as supported by the established taxonomy in [20].

The coordination mode is automatically detected by inspecting the topology of G_B , the bimanual graph produced by the combination of G_R and G_L . Each scene graph G is defined as a 3-tuple $G = (V, R, E)$, where V is the set of nodes, E is the set of edges, and R is the set of relations associated with each edge. Thus, G_B can be expressed as the union of G_R and G_L , i.e., $G_B = G_R \cup G_L$, where $V_B = V_R \cup V_L$, $E_B = E_R \cup E_L$, and $R_B = R_R \cup R_L$. Since G_B is associated with a specific coordination mode, denoted as c , we can express $G_B = \{V_B, R_B, E_B, c\}$. In Table I, we displayed all the possible topologies for G_B , and we detailed their features and meaning. The node connected to the hand can represent a single object o_m or a manipulated unity u_m . Dashed lines indicate optional edges. The last column reports the coordination modality c relative to each case. Regarding topology δ / η , we add that the two manipulated objects serve different roles: the reference object (o_{ref}) provides a reference for the dominant object (o_{dom}). For instance, when holding a cup with one hand and stirring it with a spoon using the other, the cup is o_{ref} , while the spoon is o_{dom} : the spoon's stirring action is indeed constrained by the cup's position. To determine o_{dom} , we compare right hand-object (*RO*) and left hand-object (*LO*) MI. The higher one indicates which hand manipulates o_{dom} .

If one hand is inactive, its corresponding graph will be empty. In this case, G_B will represent the activity of only the active hand, and c reports a *one arm* activity, i.e., just one arm will be involved in the robot execution.

C. Task Decomposition

A second step in the plan generation process involves exploiting the temporal variations of G_B to trace the sequence

TABLE I
 G_B FEATURES AND RELATIVE COORDINATION MODE

Topology	Features	Description	c
α / β	no nodes in common / same o_{bkg}	hands are independent and do not influence each other (e.g., transporting two glasses, one with each hand / relocating the two glasses on a shelf)	Uncordinated
γ	same o_m (and same o_{bkg})	hands work together to manipulate the same object (e.g., moving a box)	Synchronous
δ / η	$o_{mL} = o_{bkgR}$ or / and vice versa	the motion of one hand follows (as in a sequence) or depends on the motion of the other (e.g., holding a cup and stirring with a spoon)	Sequential

of actions performed. Specifically, we first segment the demonstrated task into Interaction Units (IUs), which are temporal blocks where the interactions between scene elements remain consistent. Then, we analyze the changes between couples of adjacent IUs to retrieve which action causes the transition.

To operate, we extract a representative graph G_l^{repr} for the l -th IU, which encodes the topology of all graphs within that IU. This graph is selected based on c and MI values to capture the relative poses of the scene elements at key moments, like grasp initiation or final object-object configuration. To compare adjacent IUs, we perform a difference operation on G_l^{repr} :

$$\text{diff } G^{\text{repr}} = \text{eff } G^{\text{repr}} - \text{prec } G^{\text{repr}} = G_{l+1}^{\text{repr}} - G_l^{\text{repr}}, \quad (2)$$

with G_{l+1}^{repr} representing the effects of hands' action and

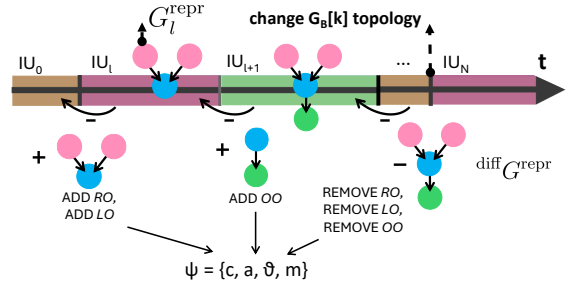


Fig. 3. Segmentation of a *synchronous* bimanual activity. Each retrieved IU is represented by its G^{repr} . Eq. (2) is applied to adjacent G^{repr} obtaining $\text{diff } G^{\text{repr}}$, which includes sub-graphs encoding new (positive sign) and ended (negative sign) interactions. Each sub-graph is mapped into high-level primitives ψ .

Algorithm 1 High-Level Primitive ψ Extraction

```

1:  $P \leftarrow \{\}$  ▷ list of primitives
2: for  $l \in [1, \text{tot}_{IU}]$  do
3:    $\text{diff } G^{\text{repr}} \leftarrow \text{Eq. (2)}$ 
4:   if  $\text{diff } G^{\text{repr}}$  reports a new RO / LO interaction then
5:      $a_{\psi_1} \leftarrow \text{move}$ 
6:      $\theta_{\psi_1} \leftarrow T_{R/L}^{o_m}$  ▷ hand-manipulated object relative pose
7:      $a_{\psi_2} \leftarrow \text{grasp}$ 
8:   else if  $\text{diff } G^{\text{repr}}$  reports an ended RO / LO interaction then
9:      $a_{\psi} \leftarrow \text{release}$ 
10:  else if  $\text{diff } G^{\text{repr}}$  reports a new OO interaction then
11:     $a_{\psi} \leftarrow \text{move}$ 
12:     $\theta_{\psi} \leftarrow T_{o_m}^{o_{bkg}}$  ▷ manipulated-background object relative pose
13:  Add all  $\psi$  to  $P$ 

```

G_l^{repr} representing the preconditions. G^{repr} contains the subgraphs corresponding to the new *RO*, *LO*, *OO* interactions (positive sign) and/or those ended (negative sign). Each subgraph is translated into one or a combination of high-level primitives, which represent robot actions required to replicate the corresponding IU variation caused by the hand movements. Each action is expressed as a 4-tuple $\psi = \{c, a, \theta, m\}$. Here, c is the coordination mode, a is the action type for the robotic arm (e.g., move, grasp, or release [26]), θ includes action parameters, and m identifies which hand executed the action for role allocation.

Fig. 3 graphically depicts how the segmentation process works for a bimanual *synchronous* activity. The first difference between the retrieved G^{repr} marks the beginning of new *RO* and *LO*. Each *HO* translates into a pair of primitives, ψ_1 and ψ_2 . As shown in lines 4-7 of Algorithm 1, $a_{\psi_1} = \text{move}$ and $a_{\psi_2} = \text{grasp}$ reflect the approach and the grasp of o_m , respectively. One of the parameters in θ_{ψ_1} is the observed relative pose between the hand and o_m , represented as a transformation matrix. The second variation between IUs is due to a new *OO* mapped into a primitive ψ with $a_{\psi} = \text{move}$, and in θ_{ψ} , $T_{o_m}^{o_{bkg}}$ encoding the observed relative pose between o_m and o_{bkg} is included (see lines 10-12). Finally, the last difference indicates the end of *RO* and *LO*. Each ending *HO* translates into a primitive for the release of o_m (lines 8-9). The end of *OO* is not treated. All the generated primitives are stored in a list P .

D. Plan Generation

Once we have the sequence of actions to perform and the roles the two arms should take for proper coordination, we finally generate the execution plan in the shape of a BT.

A BT is a directed, rooted tree structure used for managing execution flows in robotics. It comprises internal nodes for control logic and leaf nodes for actions or conditions. The root node periodically sends a *tick* signal down to its children, which execute and return a status (*SUCCESS*, *FAILURE*, or *RUNNING*) based on their outcomes. BTs include four standard types of control nodes (sequence, fallback, parallel, decorator), which handle the call to their children according to diverse policies as detailed in Table II, and two types of execution nodes (condition, action), whose symbols and return status are listed in Table III.

To automatically create the BT for replicating human activities, the ordered primitives in P are analyzed one by one. The first step involves checking the value of c_{ψ} to identify the coordination mode. Whenever c_{ψ} changes, a new control node is added to the root node, which starts a new subtree (referred

TABLE II
BT CONTROL NODES AND RELATIVE USE CASES

Type	Symbol	Children Call	Use Case
Sequence	\rightarrow	One after another (sequential)	Ordered actions (e.g., grasp <i>if success then move</i>)
Fallback	?	One after another (sequential)	Selector behavior (e.g., try primary instruction <i>if fail then try alternative</i>)
Parallel	\rightarrow	All at once (concurrent)	Simultaneous actions (e.g., move <i>both</i> the arms to different targets)
Decorator	\diamond	Custom	Custom

TABLE III
BT EXECUTION NODES AND RETURN STATUS

Type	Symbol	Success	Failure	Running
Action	\square	Upon completion	Impossible to complete	During execution
Condition	\circ	True	False	Never

to as *sBT*) containing the instructions required for that specific coordination mode. These subtrees are named according to c_{ψ} (*sBT_{one-arm}*, *sBT_{uncoo}*, *sBT_{sync}*, and *sBT_{seq}*) and assume different structure. Then, the value of a_{ψ} is considered. In case $a_{\psi} = \text{grasp}$ or $a_{\psi} = \text{release}$, ψ is converted into an action node which handles commands for closing or opening the robot gripper, respectively, and is added as a child node to the initiated *sBT*. When $a_{\psi} = \text{move}$, a further *sBT* (namely, a sub-subtree) is generated and attached to the initiated structure, including the action node handling the trajectory computation and execution. The value of m_{ψ} determines to which of the two arms (named arm_x and arm_y) the action node is allocated. In the graphical BT representations, we indicate action nodes assigned to arm_x with dark gray blocks and those to arm_y with light gray blocks. In the following, we describe the *sBT* corresponding to each coordination mode.

1) *One arm Subtree*: The *sBT_{one-arm}* has as root a sequence node. The typical structure for this subtree is illustrated within the blue box of Fig. 4. One arm is commanded to reach and grasp $o_{m,i}$, move towards o_{bkg} , interact with o_{bkg} following a specific motion pattern, and release $o_{m,i}$. Let us consider a wiping task where the arm is instructed to use a sponge to clean a surface: the robot first grasps the sponge, moves it close to the surface, and then executes the wiping motion based on the specific demonstrated pattern. After completing the task, the sponge is returned to its original position. As shown, *sBT_{move to o_{m,i}}*, framed in the red box, acquires and stores the pose of $o_{m,i}$ (the sponge in our example). The *at o_{m,i}* condition node uses this data to verify that the end-effector is not already at the target before initiating the trajectory. The *execute trajectory to o_{m,i}* action node uses the stored pose, along with $T_h^{o_{m,i}} \in \theta_{\psi}$, to generate and follow the required trajectory, as detailed in [22]. A similar subtree *sBT_{move to o_{bkg}}* is created to handle $o_{m,i}$ relocation movement (in our case, moving the sponge close to the surface to be cleaned), while *sBT_{move o_{m,i}}* handles the wiping motion. The dashed border around this node indicates that our pipeline currently recognizes complex motions like wiping, and the execution plan structure is set up to include them. However, these movements must be learned separately and then integrated in the BT.

2) *Uncoordinated Subtree*: In the case of *uncoordinated* activities, where the two manipulators should perform different and unrelated tasks concurrently, the *sBT_{uncoo}* consists of a father parallel node with two *sBT_{one-arm}* as children: one containing instructions for arm_x and the other for arm_y (see blocks colored with the two gray shades in Fig. 4). In this case, arm_x manipulates object $o_{m,i}$, while arm_y handles $o_{m,j}$, without interference. The parallel node allows concurrent execution by two arms but does not ensure perfect synchronization, as this is unnecessary for the bimanual activity under consideration. In the specific scenario where one or both hands hold an object

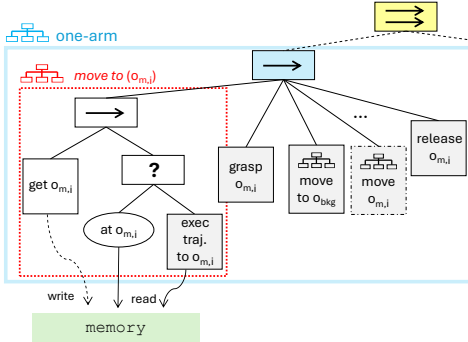


Fig. 4. Subtree for *uncoordinated* dual-arm activities, detailing the structure of *one arm* subtree in the blue box. The subtree handling movements towards a target object is detailed as well, in the red box.

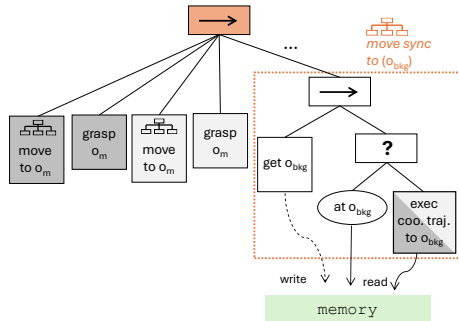


Fig. 5. Subtree for a *synchronous* dual-arm activity.

without moving it, the corresponding $sBT_{one-arm}$ will feature a *keep grasp* action node, directing the arm to maintain its grip.

3) *Synchronous Subtree*: For a dual-arm *synchronous* activity, like relocating a tray with both hands, the sBT_{sync} is structured as illustrated in Fig. 5. A single sequence node manages the commands for both arms to reach and grasp o_m at distinct grasping points, replicating the human demonstration. The color-coded blocks, in two shades of gray, always indicate the allocation. However, the peculiarity of sBT_{sync} consists in the design of the action node *exec coordinated trajectory to o_{bkg}* within the $sBT_{move sync to o_{bkg}}$, which commands both the arms to move coordinately. This action node receives the current pose of o_{bkg} relative to the camera frame ($T_{o_{bkg}}^{cam}$) and the desired final pose of o_m in θ_y as $T_{o_m}^{o_{bkg}}$. The target pose for o_m is computed by multiplying these matrices, and a trajectory is generated for o_m to reach this target pose. Each trajectory point is mapped to each arm reference frame, creating two rigidly constrained trajectories that maintain a fixed distance between the end-effectors during manipulation. These trajectories are sent to the respective controllers in a synchronized, point-by-point manner. Unlike the typical *exec trajectory to o_{bkg}* action node, where the trajectory for o_m is planned directly in the elected robot's base frame, here, it is initially planned in the camera frame and then projected onto each arm base.

4) *Sequential Subtree*: In *sequential* bimanual activities, such as holding a pot with one hand and putting the lid on it with the other, sBT_{seq} has the structure shown in Fig. 6 (a). The parent is a parallel node, with two $sBT_{one-arm}$ as children, but unlike sBT_{uncoo} , these subtrees are interdependent. Indeed, the $sBT_{one-arm}$ that instructs the arm to handle the dominant object o_{dom} (e.g., the lid) includes $sBT_{move to o_{ref}}$, which computes and executes the trajectory towards the reference object o_{ref}

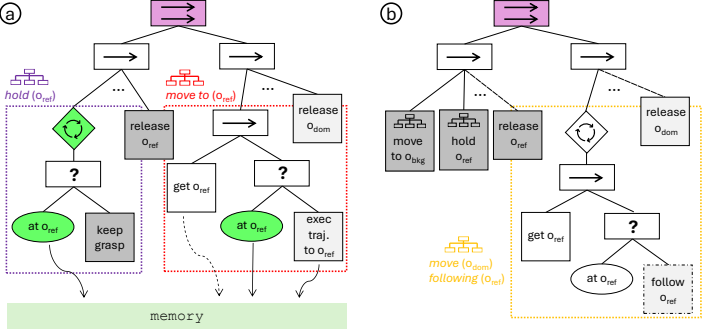


Fig. 6. Subtree for a *sequential* dual-arm activity, when the reference object is held stationary (a) and when is moved (b).

(e.g., the pot) which is held by the other arm. Thus, the other $sBT_{one-arm}$ has $sBT_{hold o_{ref}}$ to hold o_{ref} . A decorator node of type *KeepRunningUntilSuccess* ensures that the *keep grasp* command is repeatedly executed until the condition *at o_{ref}* is met, which occurs once the trajectory of o_{dom} is complete. Moreover, the main difference with sBT_{uncoo} is that, although the two arms operate simultaneously thanks to the parallel node, they have the same condition for completing their activities, allowing temporal coordination of the two arms. When such a condition is met, the *sequential* activity could terminate with a simultaneous release command, making both end-effectors ready for new instructions. If o_{ref} is not just held stationary but moved towards a target object o_{bkg} , the activity of the arm handling o_{dom} would be represented by $sBT_{move o_{dom} following o_{ref}}$, as illustrated in Fig. 6 (b). The decorator node ensures that the detection of o_{ref} and the adjustment of o_{dom} trajectory towards o_{ref} occur in a continuous loop until *at o_{ref}* is satisfied.

III. EXPERIMENTS

In our experimental campaign, we evaluated the performance of our pipeline in recognizing arms coordination mode, extracting primitive sequences, and generating effective BTs for successful task replication. We first processed multi-subject video demonstrations from our open-source dataset. These tasks, designed to highlight the defined coordination modes, were conducted in a controlled environment with subjects following instructions. Next, we tested the method on an external publicly available dataset to demonstrate its effectiveness on non-customized tasks. Additionally, we compared our bimanual task representation with that of [17].

A. Pipeline Assessment using HANDSOME Dataset

We tested our framework by processing videos of bimanual activities from our dataset HANDSOME¹. We recorded demonstrations from ten subjects using an Intel RealSense D435i camera positioned above the workspace. A marker-based system was employed to accurately detect the 6D poses of both objects and hands over time². This dataset comprehends bimanual tasks performed in two contexts (kitchen and workshop), using objects typical of each scenario. Table IV shows the instructions given to the participants for carrying out the tasks. We processed

¹The multimedia attachment related to this experimental phase is in the additional materials and online at <https://youtu.be/RZngyFtoOoE>.

²All details regarding the data recording procedure, the adopted objects, and the subjects involved are included in the open-source documentation at doi.org/10.5281/zenodo.13846970.

TABLE IV
BIMANUAL ACTIVITIES IN HANDSOME DATASET

Task	Kitchen	Workshop
1	put <i>cup</i> ₁ on <i>plate</i> ₁ then put <i>cup</i> ₂ on <i>plate</i> ₂	simultaneously put <i>profile</i> _{B1} on <i>blue ink</i> and <i>profile</i> _C on <i>yellow ink</i>
2	co-transport <i>pan</i> on <i>cooker</i>	co-transport <i>box</i> on <i>workstation</i>
3	put <i>pan</i> on <i>cooker</i> with one hand and hold it; put <i>cover</i> on <i>pan</i> with the other hand	put <i>joint</i> on <i>workstation</i> with one hand and hold it; grasp <i>profile</i> _A with the other and assemble it with <i>joint</i> ; co-transport the assembly on <i>scale</i>

all 150³ collected videos, analyzing the quality of both the segmentation and the generated BT. Since our method is one-shot, meaning we can generate an execution plan from a single demonstration, we selected one video per task and executed the generated BT using our dual-arm robotic system, consisting of two Franka Emika Panda robots placed side by side (named *franka A* and *franka B*). For the replica, we used an Intel RealSense D435i camera above the workspace to retrieve the initial object poses. The software architecture, developed in Python, ran on Ubuntu 20.04 on an Alienware laptop with an Intel i7 processor, NVIDIA RTX 2080 GPU, and 32 GB RAM.

B. Pipeline Assessment and Comparison with a State-of-the-art approach using The KIT Bimanual Dataset

To measure the effectiveness of our algorithm in processing even non-customized tasks, we additionally validated it by processing data from an external dataset of bimanual activities (The KIT Bimanual Dataset); we tested the quality of the retrieved segmentation and the generated BTs. We selected the pouring task, which was performed 10 times by 6 subjects, taking only those repetitions where the scene contained just one instance for each object category to ensure consistent object tracking. In addition, we compared the pouring task representation resulting from our segmentation with the one obtained in [17] using the same dataset.

IV. RESULTS

A. Pipeline Assessment using HANDSOME Dataset

For all demonstrations of Task 1 in the workshop context, the *uncoordinated* mode was recognized as expected, due to the two hands operating at the same time. Fig. 7 shows the video processing results (left) and robotic replica (right) of one performance. The participant simulated marking two aluminum profiles (*B1* and *C*) simultaneously with different inks (blue and yellow). The scene graphs highlighted interactions between each hand and the profiles, and between the profiles and the corresponding ink ($k = 72$, $k = 106$), with no shared nodes between graphs G_R and G_L (topology α) defining an *uncoordinated* activity. The generated BT instructed the two robots to parallel perform pick-and-place activities, as shown by the two rainbow lines depicting profile trajectories over time (see Fig. 7(right)).

Contrarily, Task 1 in the kitchen scenario was performed by first moving one cup with one hand and then the other cup with the other hand. Therefore, the two activities were recognized as *one arm*, and the BT featured a sequence of two similar $sBT_{one-arm}$, commanding the relocation of one cup and, once completed, the relocation of the other.

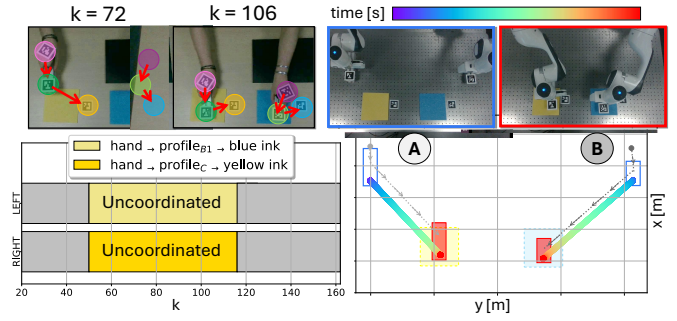


Fig. 7. (Left) Keyframes and segmentation of Task 1 in the workshop context, and (right) the robot replica. Blue and yellow squares represent the two ink sources. Profiles are drawn in blue at the start of task execution and in red at the end, with the same colors used as frame contours to illustrate object and robotic arm configurations at those moments. Gray dots indicate the end effectors' homing positions (light gray for *franka A* and dark gray for *franka B*), with dashed gray lines for their trajectories and colored trails for profiles.

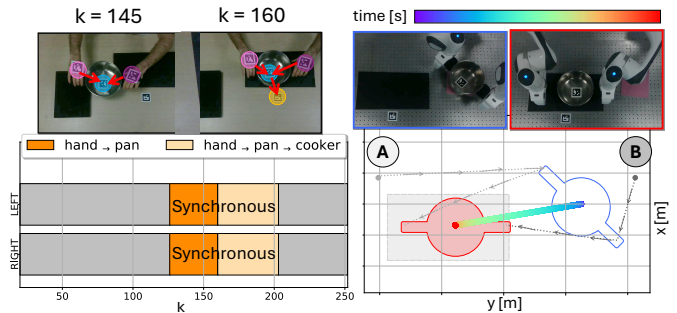


Fig. 8. (left) Keyframes and segmentation of Task 2 in the kitchen context and (right) robot replica. The gray rectangle is the cooker, while the pan is in blue at the start of the execution and in red at the end.

Across both contexts, the algorithm identified the co-transport activity in Task 2 as *synchronous* in all the demonstrations. Processing results of one performance in the kitchen context are illustrated in Fig. 8(left). The subject used both hands to grasp the pan by the handles and place it on the induction cooker. The graphs G_R and G_L were merged into a single G_B since both hands interacted with the same object, the pan. Initially, G_B only included *RO* and *LO* ($k = 145$), and later the pan-cooker interaction was detected ($k = 160$). Two distinct IUs, representing pan transport and positioning, were identified (highlighted with different orange shades). Since all G_B shared the same topology (γ), the IUs were labeled as *synchronous*. The robot replica results in Fig. 8(right) show both arms independently grasping the handles and moving the pan to the cooker via a coordinated trajectory. The BT guiding this replica consisted of a single sBT_{sync} that instructed the two arms to grasp the pan, move together, and then release it. In some instances, *RO* was detected before *LO* (and vice versa), resulting in an initial $sBT_{one-arm}$ commanding one arm to reach and grasp the pan, while the other instructions remained in sBT_{sync} . Similarly, in a few demonstrations, *RO* and *LO* did not end simultaneously, resulting in a final $sBT_{one-arm}$ including the release command for one arm. Despite slight variations in BTs, the system consistently completed the task successfully.

For all demonstrations of Task 3 in the kitchen context, the segmentation is the one shown in Fig. 9(left), as the participants were instructed on how to perform the task. First, the left hand grasped and moved the pan on the cooker, generating two IUs

³Each participant completed 3 different tasks, each repeated 5 times.

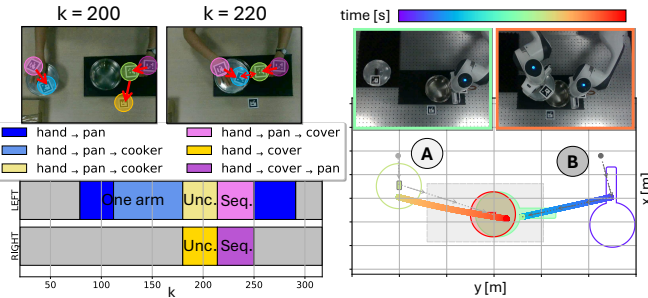


Fig. 9. (Left) Keyframes and segmentation of Task 3 in the kitchen context, and (right) the robot replica. Frame contour colors indicate object configurations: aquamarine for when the pan is on the cooker, and orange for when the cover reaches the pan. The gray rectangle represents the cooker. The pan appears in violet at the start of the task and in aquamarine once on the cooker. The cover is shown in green at the start of manipulation and in red at the end.

labeled as *one arm* since the right hand was stationary. When the right hand started manipulating the cover and the left hand maintained the grip on the pan, both G_R and G_L were created (see $k = 200$), G_B assumed topology α , and this IU was labeled *uncoordinated*. As the cover approached the pan, it resulted in a G_B of topology η ($k = 220$), and the IU was recognized as *sequential*, with the pan as o_{ref} and the cover as o_{dom} , since $MI_{R,cover} > MI_{L,pan}$. The final IU was labeled *one arm* after the right hand released the cover and moved away, leaving only G_L . During replication (see Fig. 9(right)), *franka B* acted as the left hand by moving the pan on the cooker and keeping it grasped while *franka A* placed the cover on top.

In the workshop variant of this task, the *sequential* activity was detected properly during the assembly of the two pieces. When the two hands moved the assembly together onto the scale, the coordination mode correctly switched to *synchronous*.

B. Results on The KIT Bimanual Dataset

1) *Pipeline Assessment*: We selected one demonstration from subject 2 as a representative execution (see Fig. 10(a)) and presented the segmentation results in Fig. 10(d). During the pouring phase, G_B had the topology shown for $k = 70$, and the activity was classified as *sequential*, with the bottle as o_{dom} and cup as o_{ref} , since $MI_{L,bottle} > MI_{R,cup}$. While the left hand placed the bottle on the table, the right hand held the cup: G_R and G_L remained separate, as seen at $k = 95$, labeling the IU as *uncoordinated*. In the drinking phase, only the right hand was active (see $k = 120$), then the activity required *one arm* only. Fig. 11 illustrates the BT generated from our segmentation. The *sequential* IU was mapped into a couple of interdependent subtrees triggered by the parallel node in violet, while the *uncoordinated* IU into two independent subtrees called by the parallel node in yellow. The two *one arm* IUs became two $sBT_{one-arm}$. Since each subject performed the pouring activity in their own way, we obtained diverse segmentation results and BTs. Specifically, we observed that: (i) the hand manipulating the bottle changed, but we were always able to recognize the bottle as o_{dom} ; (ii) sometimes the bottle was not released once relocated, resulting in a longer *uncoordinated* activity including the drinking motion; (iii) in some videos, subjects started lifting both cup and bottle at the same time, which resulted in an *uncoordinated* IU before the *sequential* one; (iv) in some repetitions the person switched the cup from one

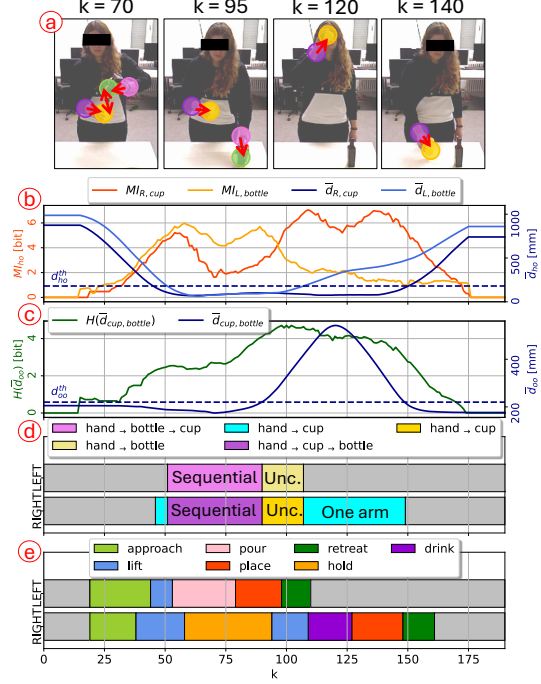


Fig. 10. (a) Keyframes of a pouring activity from The KIT Bimanual dataset; (b) trend of mutual information and average distance between each hand and the manipulated object; (c) trend of cup-bottle average distance and entropy; (d) segmentation obtained by processing the demonstration with our method and (e) with the method proposed in [17].

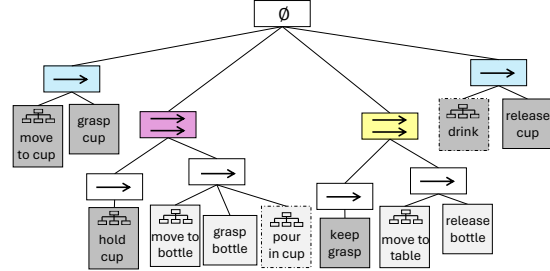


Fig. 11. The BT generated based on our segmentation of pouring activity. The colored control nodes initiate a subtree with a new coordination mode.

hand to the other to perform both pouring and drinking with the same hand. Our system does not handle this handover between hands, but we could address it by adding instructions for releasing the cup with one arm and grasping it with the other. Note that we encountered some issues in running our pipeline when positional data were very noisy due to the bad detection of the hands or when more than one instance of the same object was erroneously detected.

2) *Comparison with Bimanual Task Representation in [17]*: Clear differences can be observed between our segmentation (Fig. 10(d)) and the one obtained using the method from [17] (Fig. 10(e)). The latter is more descriptive than ours from a semantic point of view and effectively communicates the activity content to a person, using natural language labels (like *approach*, *pour*, *drink*). However, these details do not aid in the automatic generation of a plan; rather, they reduce its interpretability for a robot. Additionally, [17] returns actions for each hand separately while ignoring whether and how the two hands are coordinating. Based on this representation, the generation of a plan involving specific coordination policies between the two arms becomes more complex, as in the

pouring action. In contrast, our method identified the hand coordination strategy employed during the demonstration and automatically created a plan to replicate it, shown in Fig. 11. Fig. 10(b) and (c) also show the information-theoretic metrics calculated throughout the human performance to drive interaction detection and task segmentation, as described in [22]⁴. Specifically, $MI_{R,cup}$, $MI_{L,bottle}$, and the average distances $\bar{d}_{R,cup}$ and $\bar{d}_{L,bottle}$ were used to guide HO detection. Meanwhile, $\bar{d}_{cup,bottle}$ and its entropy $H(\bar{d}_{cup,bottle})$ guided OO detection. By analyzing $MI_{R,cup}$ and $MI_{L,bottle}$ trends, we can obtain low-level information about the motion patterns of the manipulated objects. For instance, we can distinguish between broad movements, like relocating an object, and precise, confined ones, like pouring.

V. DISCUSSION AND CONCLUSION

In this paper, we presented an intuitive programming method for dual-arm robotic systems based on single demonstrations of bimanual activities recorded using standard RGB cameras. By leveraging Shannon's information theory and the properties of scene graphs, the video processing was able to generate a high-level representation of the demonstrated task, identify the hand coordination strategies, and automatically generate a centralized execution plan. The experimental campaign was conducted by processing video from two sources: an internal open-source dataset, including multi-subjects demonstrations with real-world objects and realistic scenarios, and an external dataset. Our algorithm also performed well when applied to recordings from the external dataset, where the field of view and the system used to detect objects and hands varied from ours. This indicates that the proposed method is flexible and can accommodate different perception modules, provided that the position and orientation of each scene element are available. Additionally, the results proved the robustness of the proposed method in handling positional data from a markerless perception system, which tends to be less accurate. Currently, the system cannot replicate complex movements such as pouring, but the plan is prepared to instruct the system to perform these movements upon integration of trajectory learning algorithms. However, it should be recalled that the focus of our algorithm is to capture a high-level representation of the task and retrieve an appropriate robotic execution plan, while the specific motions can be integrated later based on the platform and object features.

While generating a robot plan from a single human demonstration is a strength, a natural evolution of the framework would involve analyzing multiple demonstrations to optimize the plan, such as reducing instructions or execution time. Additionally, by evaluating the platform's capabilities, we could identify bimanual tasks that could be performed with a single robot, optimizing resources. Finally, to increase versatility, future developments of our framework will allow users to engage directly and intuitively with the system to adapt and customize the generated plans through multi-modal inputs.

REFERENCES

- [1] M. Lorenzini, M. Lagomarsino, L. Fortini, S. Gholami, and A. Ajoudani, "Ergonomic human-robot collaboration in industry: A review," *Frontiers in Robotics and AI*, vol. 9, p. 813907, 2023.
- [2] H. Ravichandar, A. S. Polydoros, S. Chernova, and A. Billard, "Recent advances in robot learning from demonstration," *Annual review of control, robotics, and autonomous systems*, vol. 3, pp. 297–330, 2020.
- [3] S. Calinon, F. Guenter, and A. Billard, "On learning, representing, and generalizing a task in a humanoid robot," *IEEE Transactions on Systems, Man, and Cybernetics, Part B (Cybernetics)*, vol. 37, pp. 286–298, 2007.
- [4] Y. Guiard, "Asymmetric division of labor in human skilled bimanual action: The kinematic chain as a model," *Journal of motor behavior*, vol. 19, pp. 486–517, 1987.
- [5] C. Smith, Y. Karayiannidis, L. Nalpantidis, X. Gratal, P. Qi, D. V. Dimarogonas, and D. Kragic, "Dual arm manipulation—a survey," *Robotics and Autonomous systems*, vol. 60, pp. 1340–1353, 2012.
- [6] W. Takano and Y. Nakamura, "Real-time unsupervised segmentation of human whole-body motion and its application to humanoid robot acquisition of motion symbols," *Robotics and Autonomous Systems*, vol. 75, pp. 260–272, 2016.
- [7] C. L. Nehaniv and K. Dautenhahn, "The correspondence problem," 2002.
- [8] R. F. Reinhart, A. Lemme, and J. J. Steil, "Representation and generalization of bi-manual skills from kinesthetic teaching," in *2012 12th IEEE-RAS International Conference on Humanoid Robots (Humanoids 2012)*. IEEE, 2012, pp. 560–567.
- [9] E. Gribovskaya and A. Billard, "Combining dynamical systems control and programming by demonstration for teaching discrete bimanual coordination tasks to a humanoid robot," in *Proceedings of ACM/IEEE international conference on Human robot interaction*, 2008, pp. 33–40.
- [10] L. Pauly, "Seeing to learn: Observational learning of robotic manipulation tasks," Ph.D. dissertation, University of Leeds, 2021.
- [11] J. Liu, H. Sim, C. Li, K. C. Tan, and F. Chen, "Birp: Learning robot generalized bimanual coordination using relative parameterization method on human demonstration," in *2023 62nd IEEE Conference on Decision and Control (CDC)*. IEEE, 2023, pp. 8300–8305.
- [12] L. P. Ureche and A. Billard, "Constraints extraction from asymmetrical bimanual tasks and their use in coordinated behavior," *Robotics and autonomous systems*, vol. 103, pp. 222–235, 2018.
- [13] L. Fortini, M. Leonori, J. M. Gandarias, E. De Momi, and A. Ajoudani, "Markerless 3d human pose tracking through multiple cameras and ai: Enabling high accuracy, robustness, and real-time performance," *arXiv preprint arXiv:2303.18119*, 2023.
- [14] K. Ramirez-Amaro, M. Beetz, and G. Cheng, "Transferring skills to humanoid robots by extracting semantic representations from observations of human activities," *Artificial Intelligence*, vol. 247, pp. 95–118, 6 2017.
- [15] A. M. Zanchettin, "Symbolic representation of what robots are taught in one demonstration," *Robotics and Autonomous Systems*, vol. 166, p. 104452, 2023.
- [16] M. Diehl, C. Paxton, and K. Ramirez-Amaro, "Automated Generation of Robotic Planning Domains from Observations," *IEEE International Conference on Intelligent Robots and Systems*, pp. 6732–6738, 2021.
- [17] C. R. Dreher, M. Wächter, and T. Asfour, "Learning Object-Action Relations from Bimanual Human Demonstration Using Graph Networks," *IEEE Robotics and Automation Letters*, 1 2020.
- [18] R. Zollner, T. Asfour, and R. Dillmann, "Programming by demonstration: dual-arm manipulation tasks for humanoid robots," in *2004 IEEE/RSJ International Conference on Intelligent Robots and Systems (IROS)(IEEE Cat. No. 04CH37566)*, vol. 1. IEEE, 2004, pp. 479–484.
- [19] D. Paulius, Y. Huang, J. Meloncon, and Y. Sun, "Manipulation motion taxonomy and coding for robots," in *2019 IEEE/RSJ International Conference on Intelligent Robots and Systems (IROS)*. IEEE, 2019, pp. 5596–5601.
- [20] F. Krebs and T. Asfour, "A bimanual manipulation taxonomy," *IEEE Robotics and Automation Letters*, vol. 7, pp. 11 031–11 038, 2022.
- [21] T. R. J. Bossomaier, L. C. Barnett, M. S. Harré, and J. T. Lizier, *An Introduction to Transfer Entropy*. Springer, 2016.
- [22] E. Merlo, M. Lagomarsino, E. Lamon, and A. Ajoudani, "Exploiting information theory for intuitive robot programming of manual activities," *IEEE Transactions on Robotics*, pp. 1–17, 2025.
- [23] M. Colledanchise and P. Ögren, *Behavior trees in robotics and AI: An introduction*. CRC Press, 2018.
- [24] X. Chang, P. Ren, P. Xu, Z. Li, X. Chen, and A. Hauptmann, "A Comprehensive Survey of Scene Graphs: Generation and Application," *IEEE Transactions on Pattern Analysis and Machine Intelligence*, vol. 45, pp. 1–26, 1 2023.
- [25] A. J. Bell, "The co-information lattice," in *Proceedings of the fifth international workshop on independent component analysis and blind signal separation: ICA*, vol. 2003. Citeseer, 2003.
- [26] A. Guha, Y. Yang, C. Fermueller, and Y. Aloimonos, "Minimalist plans for interpreting manipulation actions," *IEEE International Conference on Intelligent Robots and Systems*, pp. 5908–5914, 2013.

⁴Thresholds d_{ho}^{th} and d_{oo}^{th} define the minimum distance for interaction, based on prior studies [16].